DOI: 10.1021/ic9002498

Inorganic Chemistry
Article

Thermal Decomposition Reactions as Tool for the Synthesis of New Metal Thiocyanate Diazine Coordination Polymers with Cooperative Magnetic Phenomena

Mario Wriedt, Sina Sellmer, and Christian Näther*

Institut für Anorganische Chemie, Universität zu Kiel, Max-Eyth-Strasse 2, 24098 Kiel, Germany

Received February 6, 2009

Reaction of nickel thiocyanate with pyrimidine at room temperature leads to the formation of the new ligand-rich 1:2 (1:2 = ratio between metal and ligand) compound $[Ni(NCS)_2(pyrimidine)_2]_n$ (**2**) which is isotypic to $[Co(NCS)_2(pyrimidine)_2]_n$ (**1**) reported recently. In the crystal structure, the Ni^{2+} ions are coordinated by four N atoms of pyrimidine ligands, which connect the metal centers into layers, and two N atoms of terminal bonded thiocyanato anions within slightly distorted octahedra. If the synthesis is performed under solvothermal conditions and an excess of the metal thiocyanate is used, single crystals of the ligand-deficient 1:1 compound $[Ni(NCS)_2(pyrimidine)]_n$ (**4**) are obtained. Investigations on the synthesis of this compound show that it is always contaminated with large amounts of the corresponding ligand-rich 1:2 compound **2**. In the crystal structure, the Ni^{2+} ions are coordinated by two N atoms of pyrimidine ligands, which connect the metal centers into chains, and two N atoms as well as two S atoms of μ-1, 3 bridged thiocyanato anions, which conntect these chains into layers, within a slightly distorted octahedral geometry. On heating compounds **1** and **2** transform quantitatively into the ligand-deficient 1:1 Ni compound **4** and its isotypic Co compound **3**. If nickel and cobalt thiocyanate are reacted with an excess of pyrimidine in a solvent-free reaction, discrete ligand-rich 1:4 complexes of composition $[M(NCS)_2(pyrimidine)_4]$ (M = Co **5** and Ni **6**) are obtained, which could be determined by single crystal structure analysis. In their crystal structure the metal ions are coordinated by four terminal bonded pyrimidine ligands and two terminal *N*-bonded thiocyanato anions. For the ligand-rich 1:2 and ligand-deficient 1:1 compounds magnetic measurements were performed, which reveal different magnetic properties: The 1:2 compounds show a ferromagnetic and the 1:1 compounds an antiferromagnetic ordering at lower temperatures.

Introduction

Over the last years a great effort has been focused to the synthesis and investigation of new coordination polymers, inorganic−organic hybrid compounds or metal-organic frameworks.[1] This applies especially to molecular-based magnetic compounds because of their impressive structural diversity and intriguing physical properties, as well as interesting magneto-structural correlations. The rational design of these compounds remains one of the major challenges. Judicious choice of appropriate molecular building blocks can effectively mediate the magnetic interaction between the paramagnetic metal ions and provide a powerful means to create a rich variety of new compounds with interesting magnetic properties, such as cooperative magnetic phenomena, for example, antiferro- or ferromagnetism.[2,3] The main

*To whom correspondence should be addressed. E-mail: cnaether@ac.uni-kiel.de. Phone: +49-431-8802092. Fax: +49-431-8801520.

(1) (a) Janiak, C. *Dalton Trans*. **2003**, 2781–2804. (b) Maspoch, D.; Ruiz-Molina, D.; Veciana, J. *J. Mater. Chem*. **2004**, *14*, 2713–2723. (c) Maspoch, D.; Ruiz-Molina, D.; Veciana, J. *Chem. Soc. Rev*. **2007**, *36*, 770–818. (d) James, S. L. *Chem. Soc. Rev*. **2003**, *32*, 276–288. (e) Khlobystov, A. N.; Blake, A. J.; Champness, N. R.; Lemenovskii, D. A.; Majouga, A. G.; Zyk, N. V.; Schröder, M. *Coord. Chem. Rev*. **2001**, *222*, 155–192. (f) Kitagawa, S.; Matsuda, R. *Coord. Chem. Rev*. **2007**, *251*, 2490–2509. (g) Kitagawa, S.; Uemura, K. *Chem. Soc. Rev*. **2005**, *34*, 109–119. (h) Moulton, B.; Zaworotko, M. J. *Chem. Rev*. **2001**, *101*, 1629–1658. (i) Puddephatt, R. J. *Coord. Chem. Rev*. **2001**, *216*−*217*, 313–332. (j) Robin, A. Y.; Fromm, K. M. *Coord. Chem. Rev*. **2006**, *250*, 2127–2157. (k) Batten, S. R.; Murray, K. S. *Coord. Chem. Rev*. **2003**, *246*, 103–130. (l) Blake, A. J.; Brooks, N. R.; Champness, N. R.; Crew, M.; Gregory, D. H.; Hubberstey, P.; Schröder, M.; Deveson, A.; Fenske, D.; Hanton, L. R. *Chem. Commun*. **2001**, 1432–1433. (m) Blake, A. J.; Champness, N. R.; Hubberstey, P.; Li, W.-S.; Withersby, M. A.; Schröder, M. *Coord. Chem. Rev*. **1999**, *183*, 117–138. (n) Janiak, C.; Uehlin, L.; Wu, H.-P.; Klüfers, P.; Piotrowski, H.; Scharmann, T. G. *J. Chem. Soc., Dalton Trans*. **1999**, 3121–3131.

(2) (a) Pardo, E.; Ruiz-Garcia, R.; Cano, J.; Ottenwaelder, X.; Lescouezec, R.; Journaux, Y.; Lloret, F.; Julve, M. *Dalton Trans*. **2008**, 2780–2805. (b) Liu, M. L.; Shi, W.; Song, H. B.; Cheng, P.; Liao, D. Z.; Yan, S. P. *CrystEngComm* **2009**, *11*, 102–108. (c) Drabent, K.; Ciunik, Z.; Ozarowski, A. *Inorg. Chem*. **2008**, *47*, 3358–3365. (d) Habib, H. A.; Sanchiz, J.; Janiak, C. *Dalton Trans*. **2008**, 1734–1744. (e) Gavrilenko, K. S.; Cador, O.; Bernot, K.; Rosa, P.; Sessoli, R.; Golhen, S.; Pavlishchuk, V. V.; Ouahab, L. *Chem.—Eur. J*. **2008**, *14*, 2034–2043. (f) Joel, S.; Miller, A. J. E. *Angew. Chem*. **1994**, *106*, 399–432. (g) Miyasaka, H.; Yamashita, M. *Dalton Trans*. **2007**, 399–406. (h) Prescimone, A.; Wolowska, J.; Rajaraman, G.; Parsons, S.; Wernsdorfer, W.; Murugesu, M.; Christou, G.; Piligkos, S.; McInnes, E. J. L.; Brechin, E. K. *Dalton Trans*. **2007**, 5282–5289. (i) Toma, L. M.; Lescouezec, R.; Pasan, J.; Ruiz-Perez, C.; Vaissermann, J.; Cano, J.; Carrasco, R.; Wernsdorfer, W.; Lloret, F.; Julve, M. *J. Am. Chem. Soc*. **2006**, *128*, 4842–4853. (j) Verdaguer, M.; Bleuzen, A.; Train, C.; Garde, R.; Biani, F. F. d.; Desplanches, C. *Phil. Trans. R. Soc. London Ser. A* **1999**, *357*, 2959–2976. (k) Wang, X.-Y.; Wang, Z.-M.; Gao, S. *Chem. Commun*. **2008**, 281–294. (l) Zhang, W. X.; Xue, W.; Lin, J. B.; Zheng, Y. Z.; Chen, X. M. *CrystEngComm* **2008**, *10*, 1770–1776.

Published on Web 06/15/2009

emphasis on the principle of design is to search for good bridging ligands that can effectively mediate the magnetic coupling between adjacent spin carriers. During the past decades, bridging ligands which contains azide or carboxyl groups have been widely investigated, and numerous compounds bridged by these ligands have been reported.[3,4]

In our own investigations the question if there are other small linker ligands to construct magnetic coordination polymers appears. Thiocyanates are a rational choice as azide analogues, which can coordinate terminal, in the end-to-end μ-1,3 and in the end-on μ-1,1 bridging mode. Thus, we have prepared compounds based on paramagnetic metal thiocyanates and pyrazine as N-donor ligand from which we expected compounds with interesting magnetic properties. Herein we synthesized compounds with different stoichiometric compositions: Ligand-rich 1:2 compounds of composition $[M(NCS)_2(pyrazine)_2]_n$ (M = Mn, Fe, Co, Ni) and ligand-deficient 1:1 compounds of composition $[M(NCS)_2(pyrazine)]_n$ (M = Mn, Fe, Co, Ni).[5] In the crystal structures of the ligand-rich compounds the metal cations are only connected by the pyrazine ligands into layers, whereas in the ligand-deficient compounds the metal cations are further linked by μ-1,3 bridged thiocyanato anions. Unfortunately, we only succeed in preparing the ligand-rich 1:2 compounds phase pure in solution, in which the thiocyanato anions are terminal bonded and therefore interesting magnetic exchange interactions could not be expected. But it must be noted that we succeed in preparing the ligand-deficient 1:1 compounds phase pure by thermal decomposition reactions of their ligand-rich 1:2 precursor compounds. In their crystal structure the metal centers are linked by the small sized thiocyanato anions, and therefore interesting magnetic exchange interactions could be expected. Magnetic measurements revealed that some of the ligand-deficient 1:1 compounds and interestingly some of the ligand-rich 1:2 compounds show antiferromagnetic ordering at lower temperatures, which is obviously mediated by the thiocyanato, as well as by the pyrazine bridges.

In this context we investigate if analogue coordination polymers based on metal thiocyanates and pyrimidine as N-donor ligand can be prepared. On the basis of the ligand-rich 1:2 compound $[Co(NCS)_2(pyrimidine)_2]_n$[6] reported recently, we prepared the isotypic Ni compound $[Ni(NCS)_2(pyrimidine)_2]_n$. Interestingly, corresponding ligand-deficient 1:1 compounds were not reported. This might be because these compounds cannot be prepared in solution. However, these compounds are easily accessible by thermal decomposition of their ligand-rich 1:2 precursor compounds. Moreover discrete ligand-rich 1:4 complexes were prepared like $[Mn(NCS)_2(pyrazine)_4]$[7] and $[Zn(NCS)_2(pyrazine)_4]$[8] in the pyrazine system.

In this work we report on the structural, thermal, and magnetic properties of new transition metal pyrimidine compounds with Co and Ni.

Experimental Section

Synthesis. $Ni(NCS)_2$, $Co(NCS)_2 \cdot H_2O$, and pyrimidine were obtained from Alfa Aesar. Powders of compounds **1** and **2** were prepared by stirring the reactants in water for 3 days at room temperature. The residues were filtered off and washed with ethanol and diethylether and dried in air. The purity of these compounds was checked by X-ray powder diffraction (see the Supporting Information, Figure S3) and elemental analysis.

The formation of these compounds was further investigated in solution by solvent-mediated conversion experiments, in which different ratios of the reactants were investigated (see Supporting Information). These experiments clearly show that all 1:1 and 1:4 compounds cannot be prepared phase pure in solution. We note that under hydrothermal conditions a small amount of single crystals of the ligand-deficient 1:1 Ni compound **4** can be obtained as the minor phase in a mixture with the ligand-rich 1:2 Ni **2** compound and that a small amount of single crystals of the ligand-rich 1:4 compounds **5** and **6** can only be obtained in a solvent-free reaction in a mixture with their educts.

Synthesis of poly[bis(isothiocyanato-*N*)-bis(μ_2-pyrimidine-*N*,*N'*)cobalt(II)] (1). Pink crystalline powder was prepared by the reaction of $Co(NCS)_2 \cdot H_2O$ (350.2 mg, 2.0 mmol) and pyrimidine (320.4 mg, 4.0 mmol) in 2.25 mL of water. Yield: 594.2 mg (88.6%). Calculated for $C_{10}H_8CoN_6S_2$ (335.3): C 35.82, H 2.41, N 25.07, S 19.13; found: C 35.61, H 2.44, N 24.82, S 19.16. IR (KBr): $\tilde{\nu}$ = 3415 (m), 3069 (w), 2058 (s), 1631 (w), 1592 (m), 1572 (w), 1464 (w), 1396 (m), 1212 (w), 1071 (w), 1037 (w), 812 (m), 722 (w), 700 (m), 652 (m) cm^{-1}.

Synthesis of poly[bis(isothiocyanato-*N*)-bis(μ_2-pyrimidine-*N*,*N'*)nickel(II)] (2). Blue crystalline powder was prepared by the reaction of $Ni(NCS)_2$ (349.7 mg, 2.0 mmol) and pyrimidine (320.4 mg, 4.0 mmol) in 2.25 mL of water. Yield: 587.7 mg (87.7%). Calculated for $C_{10}H_8NiN_6S_2$ (335.0): C 35.85, H 2.41, N 25.08, S 19.14; found: C 35.91, H 2.44, N 25.00, S 19.10. IR (KBr): $\tilde{\nu}$ = 3437 (m), 3095 (w), 2075 (s), 1595 (w), 1571 (w), 1464 (w), 1396 (m), 1211 (w), 1075 (w), 1028 (w), 824 (w), 723 (w), 699 (m), 656 (m) cm^{-1}.

Synthesis of poly[bis(μ_2-thiocyanato-*N*,*S*)-(μ_2-pyrimidine-*N*,*N'*)nickel(II)] (4). Single crystals were prepared by the reaction of $Ni(NCS)_2$ (87.4 mg, 0.5 mmol), pyrimidine (10.0 mg, 0.125 mmol), and 0.5 mL of water in a closed test tube at 120 °C for 3 days. On cooling green block-shaped single crystals were obtained. This compound can be prepared phase pure by thermal decomposition reaction starting from compound **2** (see Thermal Investigations).

Synthesis of Tetrakis(pyrimidine-*N*)-bis(isothiocyanato-*N*)-cobalt(II) (5). Single crystals were prepared by the solvent-free reaction of $Co(NCS)_2 \cdot H_2O$ (43.8 mg, 0.25 mmol) in pyrimidine (120.2 mg, 1.5 mmol). The reaction mixture was kept without stirring at room temperature. After 1 week pink block-shaped single crystals were obtained.

Synthesis of Tetrakis(pyrimidine-*N*)-bis(isothiocyanato-*N*)nickel-(II) (6). Single crystals were prepared by the solvent-free reaction of $Ni(NCS)_2$ (43.7 mg, 0.25 mmol) in pyrimidine (120.2 mg, 1.5 mmol). The reaction mixture was kept without stirring at room temperature. After 1 week blue block-shaped single crystals were obtained.

Elemental Analysis of the Residues Obtained in the Thermal Decomposition. (A) Isolated in the first heating step (see Thermoanalytic Investigations) for 1:2 cobalt compound **1**.

(3) (a) Abu-Youssef, M. A. M.; Escuer, A.; Mautner, F. A.; Ohrstrom, L. *Dalton Trans.* **2008**, 3553–3558. (b) Habib, H. A.; Sanchiz, J.; Janiak, C. *Dalton Trans.* **2008**, 4877–4884. (c) Li, W.; Jia, H.-P.; Ju, Z.-F.; Zhang, J. *Dalton Trans.* **2008**, 5350–5357.

(4) (a) Gruselle, M.; Train, C.; Boubekeur, K.; Gredin, P.; Ovanesyan, N. *Coord. Chem. Rev.* **2006**, *250*, 2491–2500. (b) Dong, W.; Ouyang, Y.; Liao, D.-Z.; Yan, S.-P.; Cheng, P.; Jiang, Z.-H. *Inorg. Chim. Acta* **2006**, *359*, 3363–3366. (c) Gu, Z.-G.; Xu, Y.-F.; Yin, X.-J.; Zhou, X.-H.; Zuo, J.-L.; You, X.-Z. *Dalton Trans.* **2008**, 5593–5602. (d) Triki, S.; Gomez-Garcia, C. J.; Ruiz, E.; Sala-Pala, J. *Inorg. Chem.* **2005**, *44*, 5501–5508.

(5) (a) Näther, C.; Greve, J. *J. Solid State Chem.* **2003**, *176*, 259–265. (b) Wriedt, M.; Jeß, I.; Näther, C. *Eur. J. Inorg. Chem.* **2009**, 1406–1413.

(6) (a) Lloret, F.; Julve, M.; Cano, J.; Munno, G. D. *Mol. Cryst. Liq. Cryst.* **1999**, *334*, 569–585. (b) Lloret, F.; Munno, G. D.; Julve, M.; Cano, J.; Ruiz, R.; Caneschi, A. *Angew. Chem., Int. Ed.* **1998**, *37*, 135–138.

(7) Liu, T.; Xie, Z.-P. *Acta Crystallogr.* **2007**, *E63*, m1820–m1820.

(8) Liu, T.; Xie, Z.-P. *Acta Crystallogr.* **2007**, *E63*, m1908.

Calculated for 1:1 cobalt compound **3**: C 28.24, H 1.58, N 21.95, S 25.13; found C 28.66, H 1.62, N 21.99, S 25.48. (B) Isolated in the first heating step for 1:2 nickel compound **2**. Calculated for 1:1 nickel compound **4**: C 28.27, H 1.58, N 21.98, S 25.16; found C 28.43, H 1.56, N 21.32, S 25.75.

Single-Crystal Structure Analysis. All investigations were performed with an imaging plate diffraction system (IPDS-1) with Mo Kα-radiation from STOE & CIE. The structure solutions were performed with direct methods using SHELXS-97,[9] and structure refinements were performed against F^2 using SHELXL-97.[10] For compounds **4** and **5** a numerical absorption correction was applied using X-Red[11] and X-Shape.[12] All non-hydrogen atoms were refined with anisotropic displacement parameters. All hydrogen atoms were positioned with idealized geometry and were refined with fixed isotropic displacement parameters [$U_{eq}(H) = -1.2\ U_{eq}(C)$] using a riding model with $d_{C-H} = 0.98$ Å for aromatic H atoms. Details of the structure determination are given in Table 2.

Rietveld Refinements. The structure model for the 1:2 Ni compound **2** was obtained from the isotypic 1:2 Co compound **1**[6] as well as the structure model for the 1:1 Co compound **3** was obtained from the isotypic 1:1 Ni compound **4**. The Rietveld refinements were performed using Fullprof2k with the Winplotr software package.[13] The cell parameters were first refined with WinXPOW Software package.[14] After the initial refinements of the scale factors, unit cell parameters, and profile parameters, the atomic positions were refined with soft constraints for the pyrimidine and thiocyanato ligands. All atoms were refined isotropically, and the H atoms were not considered. For difference plots of the rietveld refinements see the Supporting Information, Figures S1 and S2.

CCDC-735457 (**2**), -735458 (**3**), -735459 (**4**), -735460 (**5**), and -735461 (**6**) contain the supplementary crystallographic data for this paper. These data can be obtained free of charge from the Cambridge Crystallographic Data Centre via www.ccdc.cam.ac.uk.

X-ray Powder Diffraction (XRPD). XRPD experiments were performed using a Stoe Transmission Powder Diffraction System (STADI P) with Cu Kα-radiation ($\lambda = 154.0598$ pm) that is equipped with a linear position-sensitive detector (Delta 2 Theta = 6.5−7° simultaneous; scan range overall = 2−130°) from STOE & CIE.

Differential Thermal Analysis, Thermogravimetry, and Mass Spectroscopy (DTA-TG-MS). The heating-rate-dependent DTA-TG measurements were performed in a nitrogen atmosphere (purity: 5.0) in Al_2O_3 crucibles using a STA-409CD instrument from Netzsch. The DTA-TG-MS measurements were performed with the same instrument, which is connected to a quadrupole mass spectrometer from Balzers via Skimmer coupling from Netzsch. The MS measurements were performed in analogue and trend scan mode in Al_2O_3 crucibles in a dynamic helium atmosphere (purity: 5.0) using heating rates of 4 °C/min. All measurements were performed with a flow rate of 75 mL/min and were corrected for buoyancy and current effects. The instrument was calibrated using standard reference materials.

Elemental Analysis. CHNS analyses were performed using an EURO EA elemental analyzer, fabricated by EURO VECTOR Instruments and Software.

Spectroscopy. Fourier transform IR spectra were recorded on a Genesis series FTIR spectrometer, by ATI Mattson, in KBr pellets.

Magnetic Measurement. Magnetic measurements were performed using a Physical Property Measuring System (PPMS) from Quantum Design, which is equipped with a 9 T magnet.

Results and Discussion

Crystal Structures. The ligand-rich 1:2 compound $[Ni(NCS)_2(pyrimidine)_2]_n$ (**2**) crystallizes in the centrosymmetric orthorhombic space group *Cmca* with four formula units in the unit cell and is isotypic to the Co compound[6] reported recently. The asymmetric unit consists of one Ni^{2+} cation, which occupies the position 2/*m*, one thiocyanato anion located on a crystallographic mirror plane, and one pyrimidine ligand, which is located on a 2-fold rotation axis. The crystal structure consists of parallel sheets of square arrays of Ni^{2+} cations bridged by the bismonodentate pyrimidine ligands. Therein the Ni^{2+} cations are coordinated by four N atoms of four pyrimidine ligands and two N atoms of two terminal *N*-bonded thiocyanato anions (Figure 1: top). The Ni^{2+} cations are connected by μ-1,3 bridged pyrimidine ligands forming

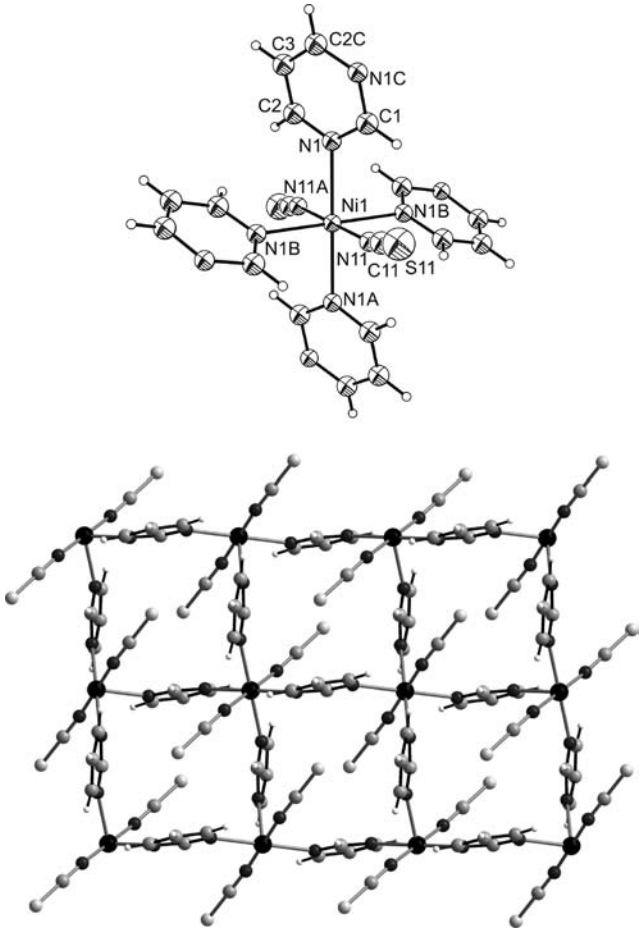

Figure 1. Crystal structure of the 1:2 Ni compound **2** with view of the coordination sphere of the Ni^{2+} cation with labeling (top) and view onto the layers of the structure in the direction of the crystallographic *b* axis (bottom). Symmetry codes: $A = -x, -y, -z$; $B = x, -y, -z + 1$; $C = -x + 1/2, y, -z + 1/2$.

(9) Sheldrick, G. M. *SHELXS-97, Program for Crystal Structure Solution*; University of Göttingen: Göttingen, Germany, 1997.
(10) Sheldrick, G. M., *SHELXL-97, Program for the Refinement of Crystal Structures*; University of Göttingen: Göttingen, Germany, 1997.
(11) *X-Red, Program for Data Reduction and Absorption Correction.*, Version 1.11; STOE & CIE GmbH: Darmstadt, Germany, 1998.
(12) *X-Shape, Program for the Crystal Optimization for Numerical Absorption Correction*, Version 1.03; STOE & CIE GmbH: Darmstadt, Germany, 1998.
(13) (a) Roisnel, T.; Rodriguez-Carvajal, J. In *WinPLOTR: a Windows tool for powder diffraction patterns analysis Materials Science Forum*, Proceedings of the Seventh European Powder Diffraction Conference (EPDIC 7), **2000**; Delhez, R., Mittenmeijer, E. J., Eds.; **2000**; pp 118−123. (b) Rodriguez-Carvajal, J. *Physica B-Condensed Matter* **1993**, *192*, 55.
(14) *WinXPOW*, Version 2.23; STOE & CIE GmbH: Darmstadt, Germany, 2003.

Table 1. Selected Crystal Data and Details on the Structure Refinement from Powder Data for Compounds **2** and **3**

compound	**2**	**3**
formula	$C_{10}H_8N_6NiS_2$	$C_6H_4N_4CoS_2$
ratio M:L	1:2	1:1
MW/g mol^{-1}	335.04	255.19
crystal system	orthorhombic	monoclinic
space group	*Cmca*	$P2_1/m$
a/Å	9.2606(1)	5.6121(3)
b/Å	16.7070(3)	12.2764(7)
c/Å	8.4154(2)	7.2074(4)
β/deg		104.40(1)
V/Å^3	1302.02(5)	480.96(5)
Z	4	2
2θ range/deg	2−70	11−60
no. reflections	173	172
no. parameters	32	33
no. soft restrains	8	8
R_p, R_{wp}	0.126, 0.132	0.292, 0.214
GOF/χ^2	0.125	0.0350
R_{Bragg}	0.0572	0.115
R_F	0.104	0.105

layers that are perpendicular to the crystallographic *b* axis (Figure 1: bottom). The NiN_6 octahedron is markedly distorted, with two equivalent Ni−NCS distances of 1.949(6) Å and four equivalent Ni−$N_{pyrimidine}$ distances of 2.245(4) Å, while the N−Ni−N bond angles are 180° (Table 3). The metal to metal separation through the pyrimidine ligand amounts to 6.2565(1) Å while the shortest internetwork Ni−Ni separation is 9.3534(1) Å. The two *trans*-oriented pyrimidine rings are coplanar, whereas the *cis*-oriented pyrimidine rings have dihedral angles of 77.5°. All distances and angles are almost comparable to that found in $[Co(NCS)_2(pyrimidine)_2]_n$.[6]

The ligand-deficient 1:1 compounds $[Co(NCS)_2(pyrimidine)]_n$ (**3**) and $[Ni(NCS)_2(pyrimidine)]_n$ (**4**) are isotypic and crystallize in the centrosymmetric monoclinic space group $P2_1/m$ with two formula units in the unit cell (Tables 1 and 2). The asymmetric unit consists of one metal cation, which is located on a center of inversion, one pyrimidine ligand that is located on a crystallographic mirror plane and one thiocyanato anion in general position. In the crystal structure the metal cations are coordinated by only two pyrimidine ligands, two S and two N atoms of four symmetry related thiocyanato anions within a slightly distorted octahedron (Figure 2).

The Co−N and Ni−N distances range between 2.136(13)−2.320(9) Å and 2.0295(16)−2.5029(6) Å (Table 4). In contrast to the ligand-rich 1:2 compounds **1** and **2** the metal cations are each μ-1,3 bridged by two thiocyanato anions forming chains that elongate in the direction of the *c* axis. Further, these metal thiocyanato chains are connected by the pyrimidine ligands into layers (Figure 3). The metal to metal separation for **3** and **4** amounts through the pyrimidine ligand 6.1382(3) and 6.0382(4) Å, through the thiocyanato anion 5.6121(3) and 5.5882(6) Å as well as two adjacent layers are separated by 7.2074(4) and 7.1643(7) Å.

The ligand-rich 1:4 compounds $[M(NCS)_2(pyrimidine)_4]$ (M = Co **5**, Ni **6**) crystallize in the centrosymmetric monoclinic space group $P2_1/c$ with four formula units in the unit cell and are isotypic. All atoms occupy general positions. The crystal structure consists of isolated complexes, in which the cations are coordinated by

Table 2. Selected Crystal Data and Details on the Structure Determinations from Single Crystal Data for Compounds **4**, **5**, and **6**

compound	**4**	**5**	**6**
formula	$C_6H_4N_4NiS_2$	$C_{18}H_{16}CoN_{10}S_2$	$C_{18}H_{16}N_{10}Ni\,S_2$
ratio M:L	1:1	1:4	1:4
MW/g mol^{-1}	254.96	495.46	495.24
crystal system	monoclinic	monoclinic	monoclinic
space group	$P2_1/m$	$P2_1/c$	$P2_1/c$
a/Å	5.5882(6)	8.9454(5)	8.9152(6)
b/Å	12.0765(9)	12.4819(9)	12.4948(8)
c/Å	7.1643(7)	20.1588(12)	20.0048(16)
β/deg	105.280(11)	98.785(7)	98.630(9)
V/Å^3	466.40(8)	2224.4(2)	2203.2(3)
T/K	170	200	200
Z	2	4	4
D_{calc}/g cm^{-3}	1.816	1.479	1.493
μ/mm^{-1}	2.480	0.987	1.098
min/max transm.	0.6008/0.7452	0.7810/0.9262	
θ_{max}/deg	27.97	26.02	28.06
measured reflns.	5406	13647	15101
unique reflns.	1176	4156	5112
reflns. [$F_o > 4\sigma(F_o)$]	1028	3164	3987
parameter	62	281	281
R_{int}	0.0349	0.0439	0.0485
$R_1{}^a$ [$F_o > 4\sigma(F_o)$]	0.0265	0.0339	0.0367
$wR_2{}^b$ [all data]	0.0666	0.0879	0.0983
GOF	1.029	0.972	1.043
$\Delta\rho_{max}$, $\Delta\rho_{min}$/e Å^{-3}	0.465, −0.670	0.399, −0.289	0.667, −0.594

^{a} $R_1 = \sum||F_o| - |F_c||/\sum|F_o|$. ^{b} $wR_2 = [\sum w(F_o{}^2 - F_c{}^2)^2/\sum w(F_o{}^2)^2]^{1/2}$.

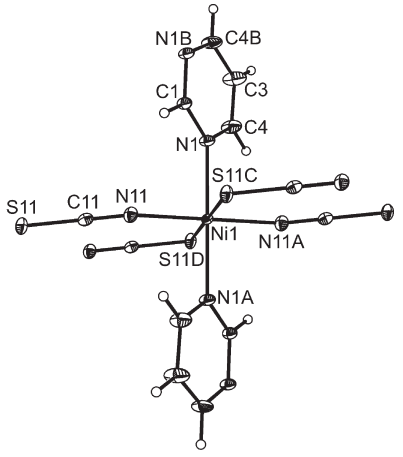

Figure 2. Crystal structure of $[Ni(NCS)_2(pyrimidine)]_n$ as representative for compounds **3** and **4** with view of the coordination sphere of the Ni^{2+} cation with labeling and displacement ellipsoids drawn at the 50% probability level. Symmetry codes: $A = -x + 2, -y + 1, -z + 2$; $B = x, -y + 3/2, z$; $C = x + 1, y, z$; $D = -x + 1, -y + 1, -z + 2$.

four pyrimidine ligands and two thiocyanato anions within slightly distorted octahedra (Figure 4 and Table 5). The pyrimidine rings I (N1/N2/C1−C4), II (N11/N12/C11−C14), III (N21/N22/C21−C24), and IV (N31/N32/C31−C34) are nearly perpendicular to each other, with dihedral angles of I/III = 77.85(8) and II/IV = 84.86(9)° for **5**, as well as I/III = 77.75(8) and II/IV = 86.59(8)° for **6**.

Investigations on the Thermal Decomposition Reactions. On heating, the ligand-rich 1:2 compounds $[M(NCS)_2(pyrimidine)_2]_n$ (M = Co[6] **1** and Ni **2**) in a thermobalance to 500 °C, two well resolved mass steps are observed in the TG curve that are accompanied with endothermic events in the DTA curve. From the MS trend scan curve, it is proven that only pyrimidine ($m/z = 80$) is emitted during these mass steps (Figure 5). The experimental mass losses

Table 3. Selected Bond Lengths [Å] and Angles [deg] for the 1:2 Ni Compound **2**

Ni(1)−N(1)	2.245(4)	Ni(1)−N(11)	1.949(6)
N(11)−Ni(1)−N(11A)	180.0	N(1)−Ni(1)−N(1A)	180.0
N(11)−Ni(1)−N(1)	89.92(16)	N(11)−Ni(1)−N(1A)	90.12(15)
N(11)−C(11)	1.206(8)	C(11)−S(11)	1.636(7)
Ni(1)−N(11)−C(11)	156.7(6)	N(11)−C(11)−S(11)	178.7(7)

Table 4. Selected Bond Lengths [Å] and Angles [deg] for the 1:1 Co **3** and Ni Compound **4**

compound	**3**	**4**
M(1)−N(1)	2.320(9)	2.138(2)
M(1)−N(11)	2.136(13)	2.030(2)
M(1)−S(11C)	2.536(5)	2.503(1)
N(1)−M(1)−N(1A)	180.0	180.0
N(11)−M(1)−N(1A)	87.3(9)	89.47(6)
N(11)−M(1)−N(1)	92.7(9)	90.53(6)
N(1)−M(1)−S(11C)	86.6(9)	89.91(5)
N(1)−M(1)−S(11D)	93.4(9)	90.09(5)
N(11A)−M(1)−S(11D)	82.0(9)	85.58(5)
N(11)−M(1)−S(11D)	98.0(9)	94.42(5)

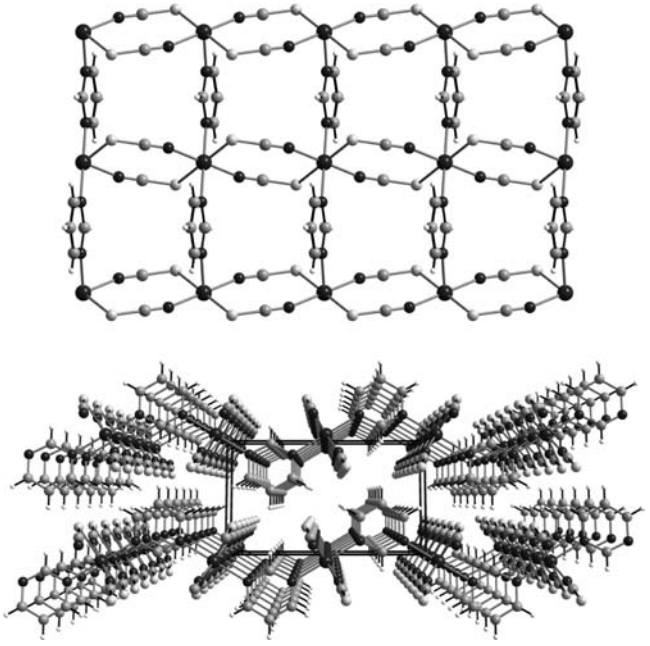

Figure 3. Crystal structure of $[Ni(NCS)_2(pyrimidine)]_n$ as a representative for compounds **3** and **4** with view onto the layers along the *c* axis (top) and view onto two adjacent sheets toward the (001) plane (bottom).

of the first two events are in good agreement with that calculated for a stepwise removal of the pyrimidine ligand (see the Supporting Information, Table S1). On further heating, the remaining ligands are emitted leading to the formation of $M(NCS)_2$, which decomposes on further heating (Figure 5).

To verify the nature of the intermediates formed, additional TG measurements were performed and stopped after the first TG step. If these residues are investigated by elemental analysis (see Experimental Section) and X-ray powder diffraction it can be shown that the ligand-deficient 1:1 compounds have been formed very pure (Figure 6). Additional measurements using temperature dependent X-ray powder diffraction are in agreement with these findings and do not show any

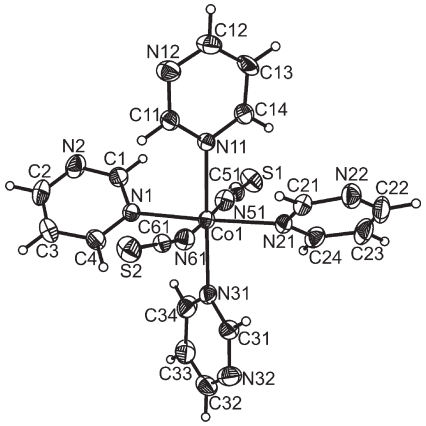

Figure 4. Crystal structure of $[Co(NCS)_2(pyrimidine)_4]$ as a representative for compounds **5** and **6** with view of the coordination sphere of the Co^{2+} cation with labeling and displacement ellipsoids drawn at the 50% probability level.

Table 5. Selected Bond Lengths [Å] and Angles [deg] for the 1:4 Co **5** and Ni Compound **6**

compound	**5**	**6**
M(1)−N(1)	2.198(2)	2.140(2)
M(1)−N(11)	2.217(2)	2.155(2)
M(1)−N(21)	2.186(2)	2.129(2)
M(1)−N(31)	2.185(2)	2.140(2)
M(1)−N(51)	2.060(2)	2.042(2)
M(1)−N(61)	2.072(2)	2.050(2)
N(1)−M(1)−N(11)	88.40(7)	88.48(7)
N(21)−M(1)−N(31)	89.64(7)	89.89(7)
N(21)−M(1)−N(1)	177.57(7)	177.62(7)
N(21)−M(1)−N(11)	89.23(7)	89.23(7)
N(31)−M(1)−N(11)	178.56(7)	178.79(7)
N(31)−M(1)−N(1)	92.74(7)	92.41(7)
N(51)−M(1)−N(61)	177.99(8)	178.34(8)
N(51)−C(51)−S(1)	179.5(2)	179.5(2)
N(51)−M(1)−N(21)	88.74(8)	88.69(7)
N(51)−M(1)−N(1)	90.70(8)	90.68(7)
C(51)−N(51)−M(1)	175.8(2)	175.9(2)
N(51)−M(1)−N(31)	90.77(8)	90.87(8)
N(51)−M(1)−N(11)	90.11(8)	89.93(7)
N(61)−M(1)−N(11)	88.47(8)	88.78(7)
N(61)−M(1)−N(1)	87.84(8)	88.24(7)
C(61)−N(61)−M(1)	164.1(2)	164.3(2)
N(61)−M(1)−N(21)	92.66(8)	92.34(7)
N(61)−M(1)−N(31)	90.69(8)	90.44(8)
N(61)−C(61)−S(2)	179.3(2)	179.4(2)

additional intermediates (see the Supporting Information, Figure S8).

Magnetic Investigations. In the ligand-rich 1:2 compounds **1** and **2**, as well as in the ligand-deficient 1:1 compounds **3** and **4**, the metal centers are μ-1,3 bridged via the aromatic pyrimidine ligands, whereas in the ligand-deficient compounds the metal centers are further μ-1,3 bridged via the small-sized thiocyanato anions. In both connection modes the metal centers are separated by only 3 atoms. Therefore cooperative magnetic phenomena might be expected, like it was observed in $[M(NCS)_2(pyrazine)_x]_n$ (M = Mn, Fe, Co, Ni; x = 1, 2) reported recently.[5,6,15] Therefore, magnetic measurements of all ligand-rich 1:2

(15) (a) Real, J. A.; Munno, G. D.; Munoz, M. C.; Julve, M. *Inorg. Chem.* **1991**, *30*, 2701–2704. (b) Haynes, J. S.; Kostikas, A.; Sams, J. R.; Simopoulos, A.; Thompson, R. C. *Inorg. Chem.* **1987**, *26*, 2630–2637. (c) Figgis, B. N.; Lewis, J.; Mabbs, F. E.; Webb, G. A. *J. Chem. Soc. A* **1967**, 442–447.

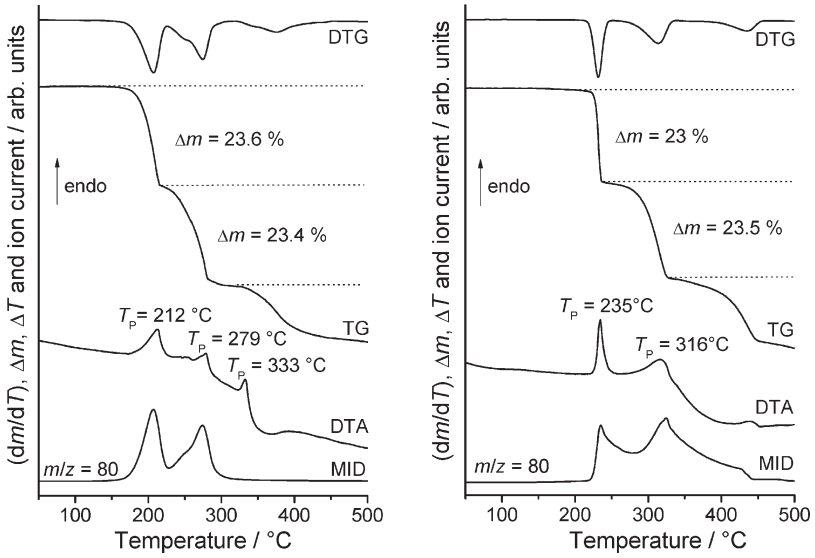

Figure 5. DTG, TG, DTA, and MS trend scan curves for the ligand-rich 1:2 compounds $[Co(NCS)_2(pyrimidine)_2]_n$ (**1**) (left) and $[Ni(NCS)_2(pyrimidine)_2]_n$ (**2**) (right). Heating rate = 4 °C/min; m/z = 80 (pyrimidine); given here are the mass changes (%) and the peak temperatures T_P (°C).

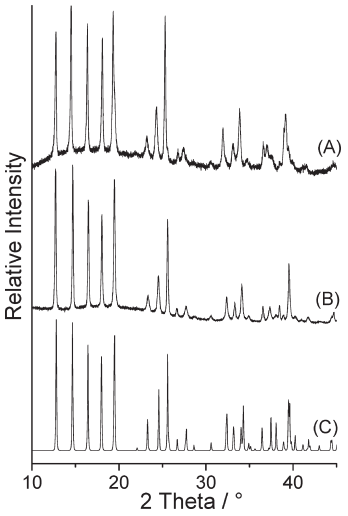

Figure 6. Experimental XRPD patterns of the residue obtained after the first TG step in the thermal decomposition reaction of the ligand-rich 1:2 compounds $[Co(NCS)_2(pyrimidine)_2]_n$[6] (**1**) (A) and $[Ni(NCS)_2(pyrimidine)_2]_n$ (**2**) (B) and XRPD pattern for the ligand-deficient 1:1 compound $[Ni(NCS)_2(pyrimidine)]_n$ (**4**) (C) calculated from single crystal data.

and ligand-deficient 1:1 compounds were performed. The magnetic susceptibility was measured as function of temperature in the range of 2−300 K, and the data were corrected for diamagnetic contributions (see Supporting Information).[16] To exclude that the results of our investigations can be regarded as due to a small amount of the reactants we additionally investigated all educts for their magnetic properties, which proves that their magnetic behavior is completely different.

For the ligand-rich 1:2 Ni compound **2** the temperature dependence of the susceptibility was investigated applying a magnetic field of $H = 1$ T (Figure 7A) and under a low applied field of $H = 0.1$ T in the temperature range of 2−30 K (Figure 7A: inset). The magnetic data between 100 to 300 K were fitted with the Curie−Weiss law $\chi_M = C/(T - \theta)$

(16) Bain, G. A.; Berry, J. F. *J. Chem. Educ.* **2008**, *85*, 532–536.

Table 6. Results of the Fits of the Magnetic Susceptibility Data with the Curie−Weiss Law for the Ligand-Rich 1:2 and Ligand-Deficient 1:1 Compounds

	1:2 compounds		1:1 compounds	
	Co **1**[6]	Ni **2**[a]	Co **3**[a]	Ni **4**[a]
C/cm^3 K mol^{-1}	3.46[a]	1.14	3.33	1.12
θ/ K	−25.43[a]	−22.48	−25.82	−16.73
μ_{eff} (exp)/μ_B	5.26[a]	3.02	5.16	3.00
μ_{eff} (calc)[20]/μ_B	3.87	2.83	3.87	2.83
$T_{ordering\ state}$/K	T_C = 8.2	T_C = 13.5	T_N = 7.1	T_N = 17.5
Fit/K	50−300	100−300	50−300	30−300

[a] This work.

yielding a negative Weiss constant $\theta = -22.5$ K (Table 6), indicating net antiferromagnetic interactions between the Ni^{2+} centers on cooling. This is also obvious by the decrease of the $\chi_M T$ values upon cooling (Figure 7B). The effective magnetic moment μ_{eff} of 3.02 μ_B is in good agreement with the spin-only value of 2.83 μ_B for a high spin Ni^{2+} ion ($S = 1$, $g = 2.0$) (Table 6). On further cooling the $\chi_M T$ curve passes a sharp maximum at $T_C = 13.5$ K suggesting a transition to the ferromagnetic state (Figure 7B). Below the maximum the $\chi_M T$ values decreases again (Figure 7B), which means that below T_C antiferromagnetic interactions seem to dominate, which may be caused by interlayer dipole−dipole exchange interactions. Furthermore, the field-cooled (FC) magnetization curve ($H = 0.1$ T) exhibits a steep increase at around $T_C = 13.5$ K, and the zero field cooled (ZFC) susceptibility curve shows a maximum at this temperature. The difference between FC and ZFC curves below the transition temperature is another hint for ferromagnetic long-range order. Note that FC and ZFC curves match perfectly above T_C. Further evidence for the ferromagnetic properties are supplied by alternating current (ac) susceptibility measurements. Both the χ_M' and χ_M'' (in-phase and out-of-phase) curves exhibit a sharp maximum at the transition temperature (Figure 7, panels D and E), a typical behavior of ferromagnetic materials. Further hint for the presence of ferromagnetic properties are provided by the magnetization saturation experiments performed at

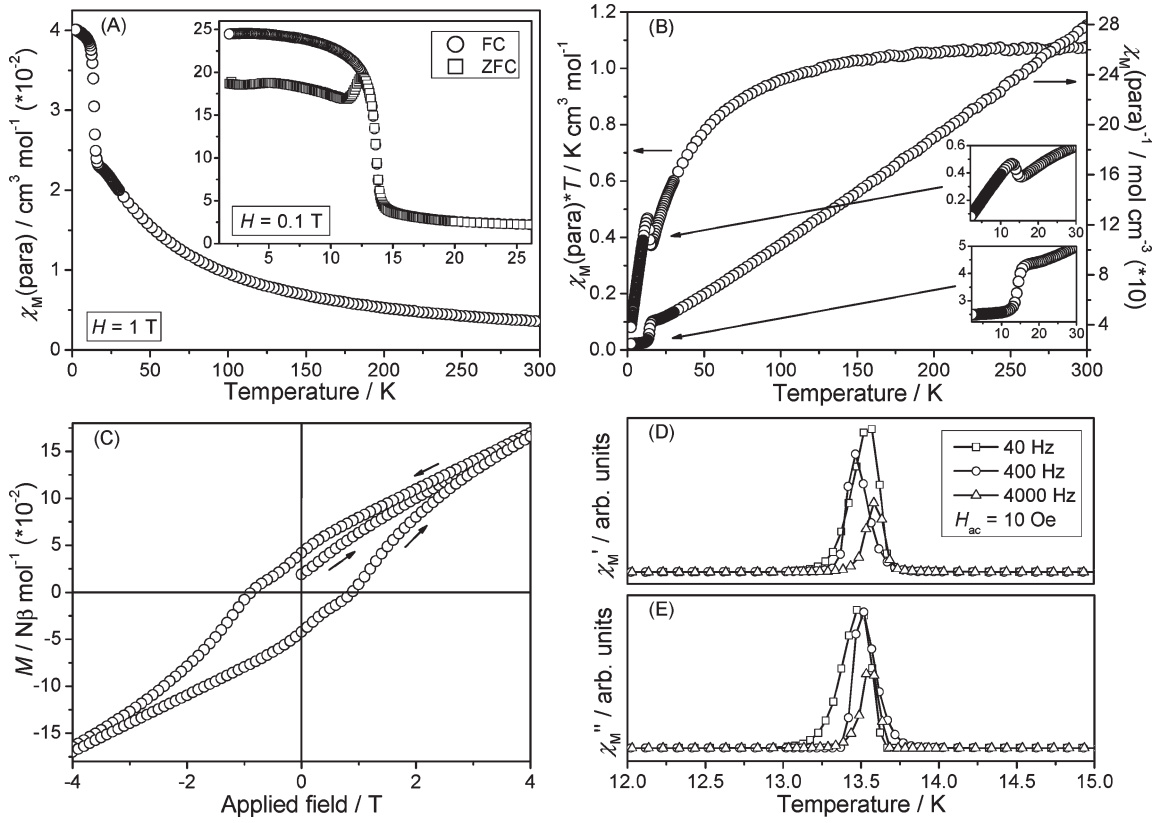

Figure 7. Results of the magnetic measurements for **2** by plots of zero-field-cooled (ZFC, at $H = 0.1$ T) and field-cooled (FC, at $H = 0.1$ and 1 T) paramagnetic susceptibility as function of temperature (A), $\chi_M T$ and reciprocal paramagnetic susceptibility as function of temperature at $H = 1$ T (B), hysteresis loop of ±4 T range at $T = 4$ K (C), and temperature dependence of in-phase χ_M' (D) and out-of-phase χ_M'' (E) ac magnetic susceptibility, $H_{ac} = 10$ Oe, 40/400/4000 Hz.

$T = 4$ K until 9 T (see the Supporting Information, Figure S9). Herein the occurrence of a hysteresis loop (Figure 7C) is typical for ferromagnetic properties, and the relatively low value for the coercitive field of $H_c = 0.9$ T and a remanent magnetization of $M_r = 0.0421$ Nβ mol^{-1} suggests soft ferromagnetic behavior. However, we cannot exclude the occurrence of metamagnetism, but our data are not fully consistent with those for a typical metamagnet. For such a behavior in most cases an increase in the $\chi_M T$ curve above T_C is observed, and the Weiss constant is commonly positive.[17]

The Co compound **1** shows a similar magnetic behavior, which is in agreement with that reported in literature.[6] It must be pointed out that the coercitive field of the Ni compound **2** is much larger than that of **1**.

Further Ni coordination polymers like the 2D networks of $[Ni(NO_2)_2]_n$[18] and [Ni(pyrimidine-4,6-dicarboxylate)]$_n$[19] and the 3D network of [Ni(4,4′-bipyridine)-$(NO_2)_2]_n$[18] show similar magnetic behavior. All these compounds have in common that their metal centers are separated by three atoms mediating a ferromagnetic transition state T_C in the same temperature range as for compounds **1** and **2**.

In contrast to the ligand-rich 1:2 compounds, the ligand-deficient 1:1 compounds **3** and **4** show a different behavior. The temperature dependence of the magnetic susceptibilities was investigated under an applied magnetic field of $H = 1$ T. A sharp maximum in the χ_M versus T curves is observed, which indicates an antiferromagnetic ordering at $T_N = 7.1$ K for **3** and $T_N = 17.5$ K for **4** (Figure 8: top). Above these ordering temperatures the χ_M^{-1} versus T curve is essentially linear following the Curie−Weiss law (Figure 8: middle). The negative Weiss constant $\theta = -25.82$ K for **3** and $\theta = -16.73$ K for **4** (Table 6) and the decrease of the $\chi_M T$ versus T curves upon cooling confirms the antiferromagnetic behavior (Figure 8: bottom). The effective magnetic moment μ_{eff} of 5.19 μ_B for **3** is larger than the spin-only value of 3.87 μ_B for a high spin Co^{2+} ion ($S = 3/2$, $g = 2.00$). But it is well documented that a significant spin−orbit coupling/zero-field splitting with g-values strongly deviating from 2.00 yields effective magnetic moments between 4.3 and 5.2 μ_B.[20] For **4** a value of 3.00 μ_B is found, which is in good agreement with the spin-only value of 2.83 μ_B for a high spin Ni^{2+} ion ($S = 1$, $g = 2.00$) (Table 6).

In summary, one can assume that the bridging pyrimidine ligands mediate the ferromagnetic ordering whereas

(17) (a) Hao, X.; Wei, Y. G.; Zhang, S. W. *Chem. Commun.* **2000**, 2271–2272. (b) Yee, G. T.; Whitton, M. J.; Sommer, R. D.; Frommen, C. M.; Reiff, W. M. *Inorg. Chem.* **2000**, *39*, 1874–1877.

(18) Vo, V.; Kim, Y.; Minh, N. V.; Hong, C. S.; Kim, S.-J. *Polyhedron* **2009**, *28*, 1150–1154.

(19) Masciocchi, N.; Galli, S.; Tagliabue, G.; Sironi, A.; Castillo, O.; Luque, A.; Beobide, G.; Wang, W.; Romero, M. A.; Barea, E.; Navarro, J. A. R. *Inorg. Chem.* **2009**, *48*, 3087–3094.

(20) Holleman, A. F.; Wiberg, E. *Lehrbuch der Anorganischen Chemie*; de Gruyter: Berlin - New York, 1995; Vol. 101.

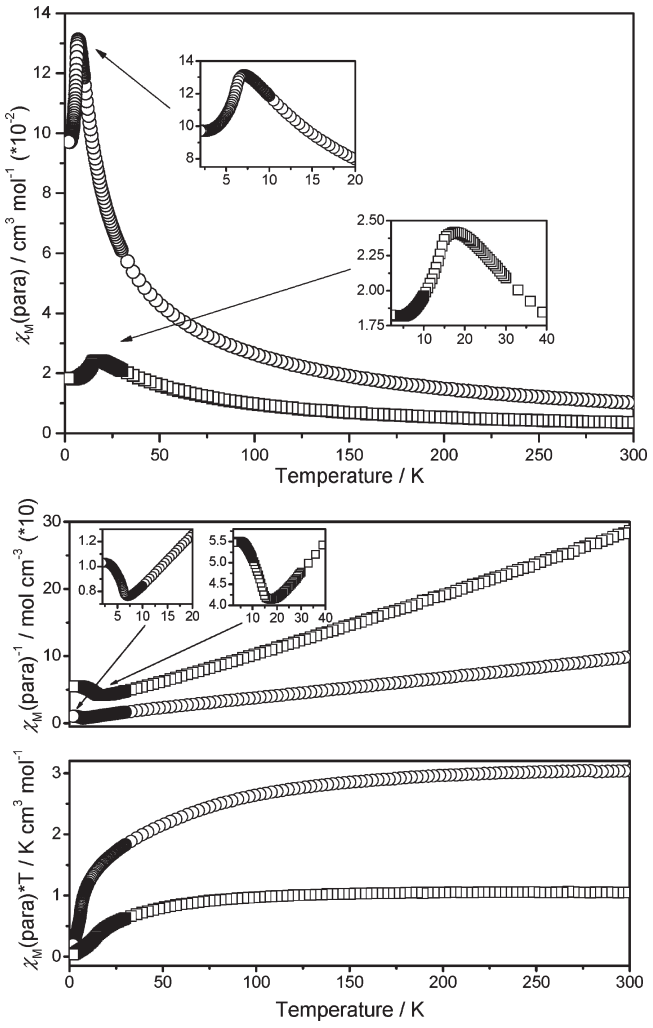

Figure 8. Results of the magnetic measurements for **3** (○) and **4** (□) by plots of field-cooled paramagnetic susceptibility as function of temperature (top), reciprocal paramagnetic susceptibility (middle), and $\chi_M T$ as function of temperature (bottom) (all at $H = 1$ T).

the bridging thiocyanato anions mediate the antiferromagnetic ordering.

Conclusion

In this contribution we have presented five new coordination polymers based on metal thiocyanates and pyrimidine ligands: Ligand-rich 1:2 and ligand-deficient 1:1 coordination polymers, as well as discrete ligand-rich 1:4 complexes. Unfortunately only the ligand-rich 1:2 compounds can be obtained phase pure in solution, whereas the synthesis of the ligand-deficient 1:1 compounds cannot. However, the latter compounds are easily accessible by thermal decomposition of their ligand-rich 1:2 precursor compounds. Therefore, we have conclusively shown that thermal decomposition reactions are an alternative tool for discovering additional ligand-deficient phases with interesting magnetic properties. One of the advantages of this method is that decompositions reactions of suitable ligand-rich precursor compounds must lead to compounds with a higher degree of condensation and different magnetic properties like those reported in this contribution. In the case of the ligand-rich 1:2 compounds the metal centers are only μ-1,3 bridged by the pyrimidine ligands, ferromagnetic ordering is observed, whereas for the ligand-deficient 1:1 compounds, in which the metal centers are further μ-1,3 bridged by the thiocyanato anions, antiferromagnetic ordering at lower temperatures appears. The structural changes of the thiocyanato anions during thermal decomposition were also proved by IR spectroscopic investigations, which is especially useful if no single crystal data are available (see Supporting Information).

However, for a better understanding of the magneto-structural correlations many more systematic investigations are needed. Thus, similar coordination polymers based on small-sized anions like thiocyanates, cyanates, and formates with N-donor ligands like pyrazine, pyrimidine, pyridazine, and 4,4′-bipyridine will be investigated in future. From such investigations, we expect to see a large number of new compounds with interesting magnetic behavior.

Acknowledgment. M.W. thanks the *Stiftung Stipendien-Fonds des Verbandes der Chemischen Industrie* and the *Studienstiftung des deutschen Volkes* for a PhD scholarship. Moreover we gratefully acknowledge financial support by the State of Schleswig-Holstein, and we thank Professor Dr. Wolfgang Bensch for the opportunity to use of his experimental facility and his helpful discussions on the magnetic investigations.

Supporting Information Available: Difference plots of the rietveld refinements from powder data of compounds **2** and **3**, experimental and calculated X-ray powder patterns of compounds **1** and **2**, IR spectra of compounds **1**−**4** and their interpretation, solvent-mediated conversion experiments of all compounds, experimental and calculated mass losses of compounds **1** and **2**, temperature-dependent XRPD investigations of the decomposition process of compounds **1** and **2**, diamagnetic increments and magnetization versus applied field plot for compound **2**. This material is available free of charge via the Internet at http://pubs.acs.org.